ACS APPLIED MATERIALS & INTERFACES

RESEARCH ARTICLE

www.acsami.org

Low-Loss, High-Permittivity Composites Made from Graphene Nanoribbons

Ayrat Dimiev,[†] Wei Lu,[†] Kyle Zeller,[‡] Benjamin Crowgey,[‡] Leo C. Kempel,[*,‡] and James M. Tour[*,†,§,⊥]

[†]Departments of Chemistry, [§]Mechanical Engineering and Materials Science and the [⊥]Smalley Institute for Nanoscale Science and Technology, Rice University, MS-222, 6100 Main Street, Houston, Texas 77005, United States

[‡]Department of Electrical and Computer Engineering, Michigan State University, East Lansing, Michigan 48824, United States

ABSTRACT: A new composite material was prepared by incorporation of graphene nanoribbons into a dielectric host matrix. The composite possesses remarkably low loss at reasonably high permittivity values. By varying the content of the conductive filler, one can tune the loss and permittivity to desirable values over a wide range. The obtained data exemplifies how nanoscopic changes in the structure of conductive filler can affect macroscopic properties of composite material.

KEYWORDS: dielectric, permittivity, loss, conductive filler, graphene nanoribbons

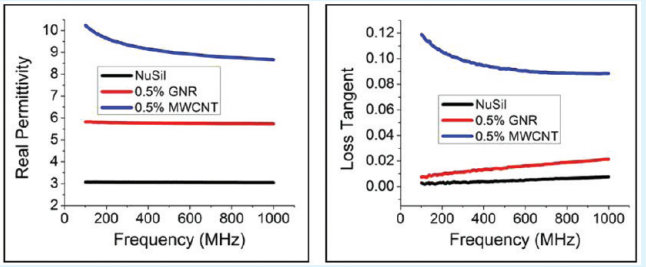

INTRODUCTION

Carbon nanotubes (CNTs) possess remarkable properties such as high aspect ratio, mechanical strength and unique electrical conductivity.[1] This facilitates their use in the fabrication of a variety of composites, which were the first major commercial applications of multiwalled carbon nanotubes (MWCNTs).[1] CNTs can interact strongly with impressed radio and microwave fields.[2−5] Both single-wall carbon nanotubes (SWCNTs) and MWCNTs can be used as conductive fillers in the synthesis of composites. Because MWCNTs have a higher performance-to-price ratio, attention is generally focused on them for composites. It is known that incorporation of CNTs into a dielectric polymer matrix significantly increases the permittivity of the resulting composite material.[3−8] Because of their high aspect ratios and high persistence length based on their tubular rigidity, very low fractions of CNTs are required to significantly increase the permittivity of a polymer. Incorporation of CNTs increases both the real and imaginary parts of permittivity and the resulting composites exhibit very high loss even at fractions as low as 0.5 wt %.[5,6,8] At the same time miniaturization of electronic components requires materials with high permittivity and low loss in the radio and low microwave frequency region.[9] In the high frequency microwave region, low loss is critical for antennas and other military applications. In this paper we show that composite materials prepared from graphene nanoribbons (GNRs)[10] possess extremely low loss values, compared to composites prepared from the parent MWCNTs, at reasonably high permittivity values. A two-part silicone elastomer (NuSil Technology R-2615) was used as the host polymer. The samples were tested in the 1−1000 MHz spectrum.

EXPERIMENTAL SECTION

The MWCNTs were provided by Mitsui & Co. and were used without further purification.

Splitting of MWCNTs to Form GNRs. The GNRs were prepared as we described previously.[10] MWCNTs (1.00 g) and potassium metal pieces (3.00 g) were placed in a 50 mL Pyrex ampule. The ampule was evacuated and sealed with a flame. The ampule was heated in a furnace at 250 °C for 14 h. The heated ampule, containing a golden-bronze-colored potassium intercalation compound, was cooled to room temperature, opened in a glovebox, and mixed with 20 mL of ethyl ether. Next, 20 mL of ethanol was slowly added into the reaction mixture. The quenched product was washed consecutively with ethanol, water, and ether and filtered through a 0.40 μm PTFE (Teflon) membrane. The as-prepared GNRs were characterized and used to make composite materials.

Production of Composite Materials. The composite materials were made using a two-part silicon elastomer (NuSil Technology R-2615, NuSil). The conductive filler (MWCNT, or GNR from 3.0 mg to 48.0 mg depending on loading) was horn-sonicated (Cole Palmer ultrasonic processor Model 750 W) for 5 min in 5 mL of chloroform to obtain a suspension. The contents of the conductive filler given elsewhere in this article are weight percentages. Separately, part A of NuSil (2.16 g) was dissolved in 10 mL of chloroform. The GNR-chloroform suspension was added to the elastomer solution and the mixture was stirred. The resulting mixture was horn-sonicated for 30 min at 30 s on/30 s off intervals. Most of the solvent evaporated during the sonication. This sequence of blending and solvent evaporation facilitated uniform dispersion of the GNRs in the polymer matrix. The high level of dispersion was not achieved by simple mechanical blending of GNRs into the NuSil. Next, the mixture was placed in a vacuum oven (10 mmHg, 60 °C) for 2 h to remove the remaining chloroform. Part B of the NuSil elastomer (0.24 g) was added into the mixture and manually stirred to mix parts A and B. The mixture was then poured into the bottom part of an appropriately shaped (see below)

Received: August 9, 2011
Accepted: November 5, 2011
Published: November 06, 2011

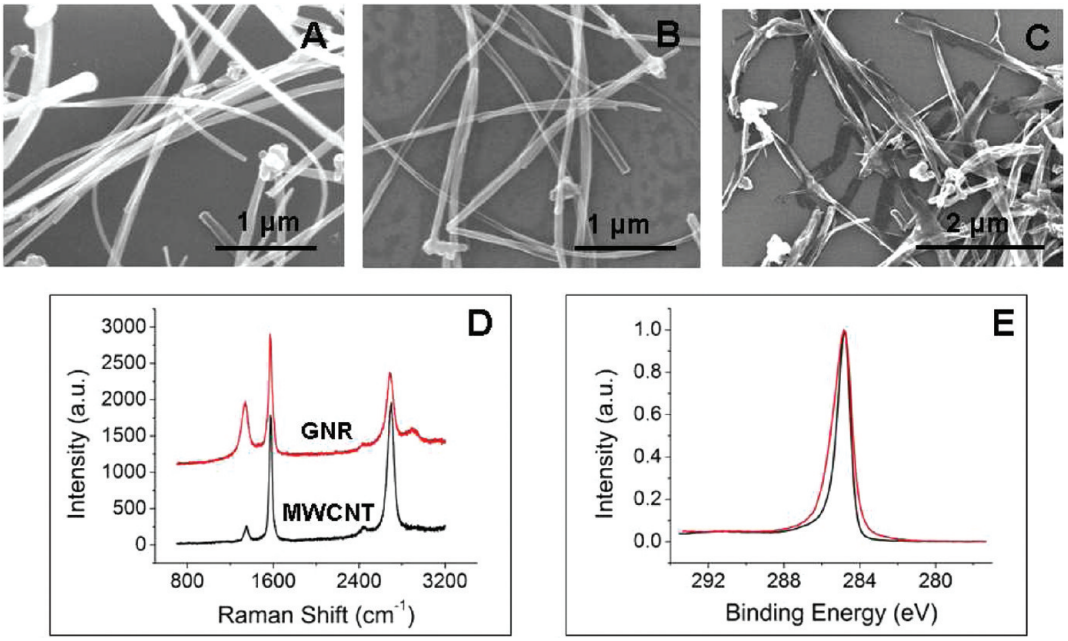

Figure 1. Characterization data for GNRs in comparison to parent MWCNTs. SEM images of (A) MWCNTs, (B) folded GNRs, and (C) GNRs unfolded in a chlorosulfonic acid and ammonium persulfate/sulfuric acid mixture. (D) Raman, and (E) C1s XPS spectra of MWCNTs (black), and folded GNRs (red).

mold, and was placed into an evacuated desiccator for 30 min to remove trapped air. The top of the mold was then placed atop and the elastomer was cured in an oven at 100 °C for 2 h.

Electrical Measurements. The permittivity and loss values were calculated from capacitance values measured with an impedance analyzer (Agilent E4991A RF). The samples were cylindrical with a diameter of 20.0 mm and the height (thickness) of 2.0 mm. To reduce the measurement uncertainty, five scans were recorded for every sample, and the average values are reported below. The 1−1000 MHz region was tested, but due to the inherent device uncertainty at low-frequency values in the Agilent E-4991A, data collected at frequencies below 100 MHz have been omitted for clarity's sake.

RESULTS AND DISCUSSION

Figure 1 shows how potassium vapor splitting changes the structure and morphology of MWCNTs (Figure 1A) into their split form of GNRs that remain coiled and foliated. As-prepared GNRs (Figure 1B) appear somewhat similar to the precursor MWCNTs but with a split extending longitudinally. Though it is difficult to distinguish the differences between the two by SEM, Figure 1C shows the same GNRs after consecutive treatments in chlorosulfonic acid followed by a treatment with a solution of ammonium persulfate in sulfuric acid. The treatment facilitates unfolding of the split tubes to produce multilayer GNRs and establishes that the structures in Figure 1B are indeed split yet folded and foliated.[10] Only the folded GNRs were used in this work for characterization and for making composite materials. The Raman spectrum of the GNRs (Figure 1D) is significantly different from the spectrum of the parent MWCNTs and is similar to that of defective graphene.[11,12] The high D peak supports the conclusion that the GNRs are disordered likely due to the new edge generation. The C1s XPS spectra of both the parent MWCNTs and the GNRs contain only one carbon peak centered at 284.8 eV (Figure 1E). Potassium splitting caused the peak to broaden in the GNR spectrum. This is the evidence for appearance of sp^3 carbons along with sp^2 carbon content.[13] Therefore, the splitting process is analogous to cutting of a rubber hose longitudinally. Similar to a split rubber hose, the GNRs maintain a cylindrical shape and the resilient properties of the parent MWCNTs. van der Waals interlayer interactions provides a sufficient barrier to their flattening and exfoliation. The GNRs are not crumpled and very few sharply bent structures are observed in the SEM images (Figure 1B). This allows the GNRs to retain their shape while being incorporated into the polymer matrix.

The complex permittivity ε consists of the real ε' and imaginary ε'' parts (eq 1).

$$\varepsilon = \varepsilon' + i\varepsilon'' \quad (1)$$

Figure 2 shows the permittivity of the NuSil based composite prepared by incorporation of as little as 0.5 wt % GNRs. The permittivity of pure NuSil and of the composite made from parent MWCNTs are given for comparison. The real permittivity of GNR/NuSil (Figure 2A) is lower than that for MWCNT/NuSil, but still at considerably high values compared with pure polymer. The high permittivity in the low-frequency region, which is the signature for all the CNT-based composites in the tested region,[6−8] is not observed for GNR/NuSil. Remarkably, the permittivity is flat across the entire tested frequency region.

As it is evident from Figure 2B the imaginary permittivity of GNR/NuSil is 1 order of magnitude lower than the one made from MWCNTs. Because the real permittivity is still high, the composite exhibits remarkably low loss tangent (ratio of imaginary to real permittivity) (Figure 2C) compare with the MWCNT/NuSil composite. The loss tangent values are 0.008 in the vicinity of 100 MHz, and 0.019 at 1000 MHz, values that were never achieved for CNT/polymer composites.[3−8]

The permittivity of dielectric materials decreases with frequency. There is always a delay in the material's response to an applied field, and at higher frequencies the material is not completely polarized

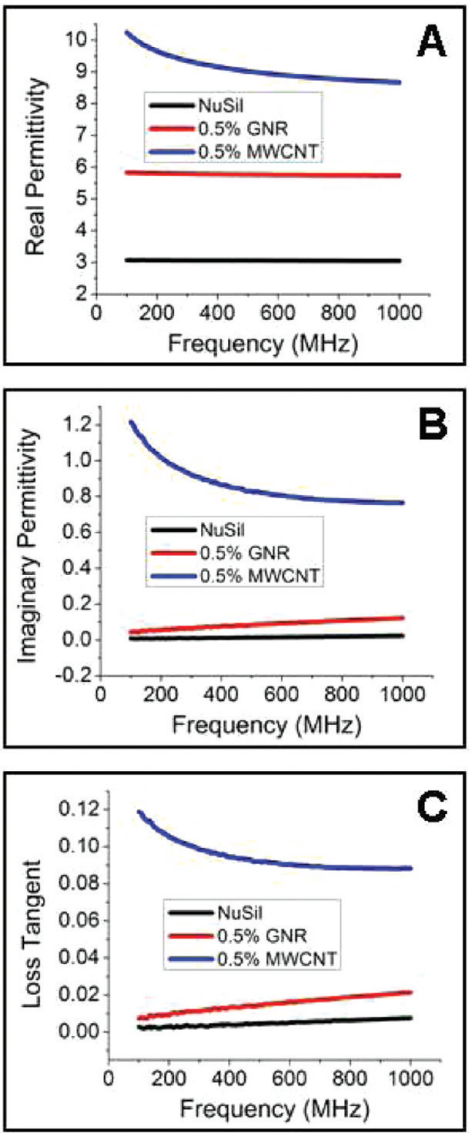

Figure 2. Dielectric properties of the GNR/NuSil composites. (A) Real permittivity, (B) imaginary permittivity, and (C) loss tangent of pure NuSil (black), MWCNT/NuSil (blue), and GNR/NuSil (red) composites containing 0.5 wt % incorporated conductive filler.

and relaxed. For composite materials containing conducting filler in the dielectric host, the change in permittivity values occurs mainly in the high-radio and low-microwave frequency region of 1×10^4 to 1×10^7 Hz. Thus at 1×10^4 Hz, permittivity values are higher than those at 1×10^7 Hz.

The permittivity of composites dramatically increases in the vicinity of the percolation threshold of conductive fillers.[14−17] This increase mainly occurs at higher loading fractions (close to percolation threshold) and is more pronounced at frequencies $<1 \times 10^3$ Hz. For the composites with low conductive filler fraction, the frequency-dependent change in permittivity is less pronounced and shifted to the lower-frequency region.[14−17]

Figure 3 shows the characteristics of GNR/NuSil composites containing different fractions of conductive filler. The real permittivity increases almost linearly with the weight percent of GNRs in the composite (Figure 3A, D). The real permittivity lines (Figure 3A) for the 0.12, 0.25, and 0.5 wt % loaded samples are flat, whereas the lines for the 1.0 wt % and 2.0 wt % samples exhibit a slight frequency-dependent slope in the low-frequency region similar to the MWCNT/Nusil composite (Figure 2A).

Interestingly, the imaginary part of the 0.5 wt % GNR/NuSil composite is extremely low (Figure 3B) and only insignificantly higher than those for the 0.12 and 0.25 wt % content composites. Furthermore, the composite with 0.5 wt % loading exhibits remarkably low loss at reasonably high permittivity. Note that even for the highly loaded samples where the permittivity is high, the loss tangent still remains at low values. The imaginary permittivity of the GNR/NuSil composites behaves differently from that of the MWCNT/NuSil composite. For the latter both real and imaginary values decrease with frequency (Figure 2A, B). For the former, the imaginary part increases with frequency in the entire tested region (Figure 3B). This occurs even for the 1.0 and 2.0 wt % loaded samples, where the real permittivity is equal to or exceeds the permittivity of the 0.5 wt % MWCNT/NuSil composite.

The macroscopic permittivity of composite material is complex. It depends on many factors such as the permittivity of the host matrix, the shape, persistence length, and conductivity of the conductive filler, the distribution of the conductive filler in the matrix, and the interfacial polarization. To assess the permittivity dependence on the distribution of conductive filler in the polymer matrix, we prepared two different samples of 0.5 wt % GNR/NuSil composites. The first was prepared with extensive sonication as described in the experimental section, whereas the other was prepared simply by manual stirring of the GNRs with the polymer. The permittivity of the two composites was different. The real permittivity value at 600 MHz for the manually blended sample was 4.0, whereas for the composite prepared with sonication, the real permittivity was 5.8. This experiment demonstrates that the distribution of the conductive filler plays an important role in the macroscopic permittivity of the composite. This impacts potential applications since the variability (batch-to-batch) in permittivity suggests that resonant applications, such as dielectric resonators, RF filters, etc., will impact device performance. Rather, nonresonant applications, such as wide bandwidth antennas, can make effective use of such materials.

Figure 4 shows images of the distribution of the GNRs in the polymer matrix. As seen from the images, the GNR foliated stacks are almost uniformly distributed in the polymer. Very few aggregates of the GNR stacks were found in the composites with 0.12−0.5 wt % loading (Figure 4A). The aggregates were very small and contained only a few GNRs as they had been stacked from the reaction. In composites with 1.0 and 2.0 wt % loading, both the number and the size of the aggregates become significant. Thus, the uniformity of the composites decreased with increasing filler content.

As it is evident from the SEM images of the GNR/NuSil composites (Figure 4), the GNRs retain their original cylindrical shape after being blended into the polymer. From this perspective, there is little difference between the shapes of individual GNRs and the precursor MWCNTs in the NuSil matrix. It is difficult to thoroughly assess any difference in the uniformity of distribution between GNRs and MWCNTs in the prepared composite samples. Both composites with 0.5 wt % loading contain areas of almost ideal distribution where single CNTs are uniformly blended into the polymer, and both composites contain some areas with aggregates. We did not observe any significant difference in the distribution of the filler between the

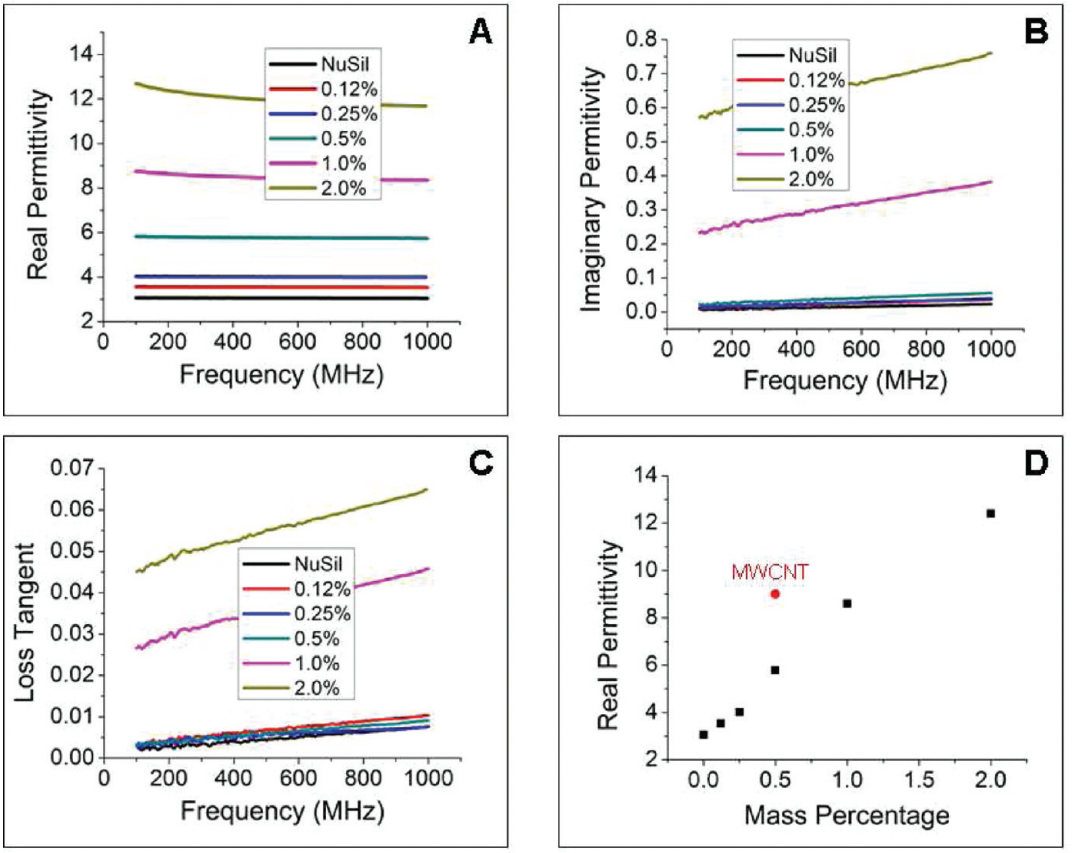

Figure 3. Electromagnetic properties of the GNR/NuSil composites at varying GNR concentrations. (A) Real permittivity, (B) imaginary permittivity, and (C) loss tangent for GNR/NuSil composites with different fractions of GNRs. (D) Real permittivity vs weight percentages measured at 600 MHz. The red dot representing the composite containing 0.5 wt % MWCNTs is shown for comparison purposes.

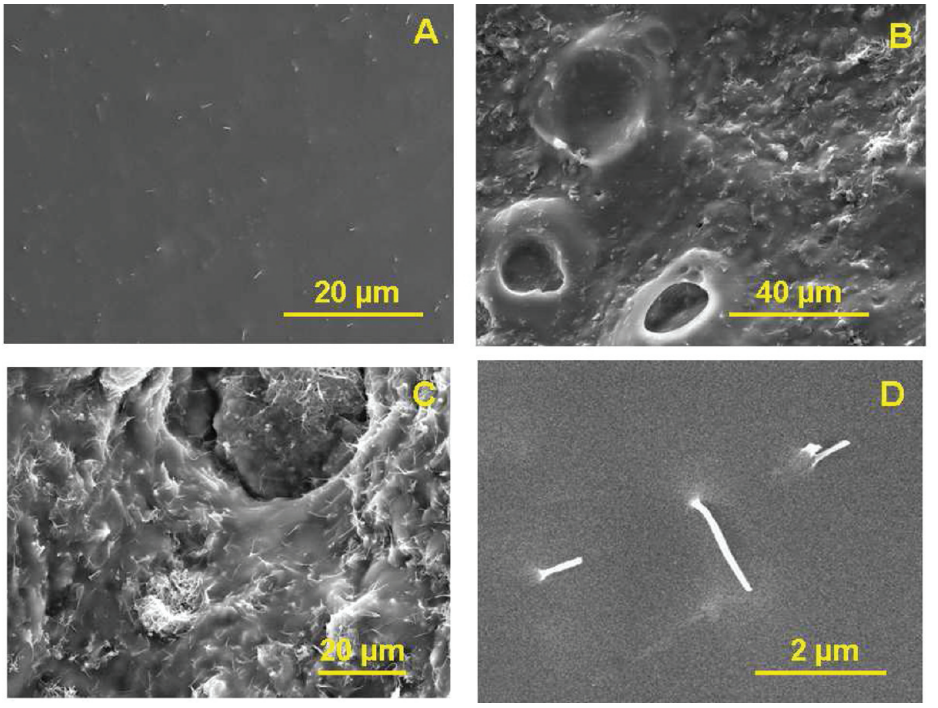

Figure 4. SEM images of GNR/NuSil composites containing different fractions of conductive filler. (A) 0.5, (B) 1.0, and (C) 2.0 wt % GNRs. (D) Higher-magnification SEM image of the 0.5 wt % GNR composite indicates that GNRs retain their original shape after being blended into the polymer.

two samples. Subsequently, on the basis of the available data, the observed change in permittivity (Figure 2) is likely due to the change in the interfacial polarization between the MWCNTs and the polymer matrix caused by splitting.

It is known that the electrical conductivities of individual MWCNTs can vary. Even MWCNTs from the same batch exhibit a difference of several orders of magnitude in conductivity.[18] This is because the MWCNTs contain both metallic and semiconducting walls with different chiralities. Since the conductivity of the metallic walls exceeds the conductivity of the semiconducting walls, the conductivity of individual MWCNTs depends on the number of metallic walls. It was recently shown that the outermost metallic wall of the MWCNT strongly diminishes the incident field inside the structure.[3] Subsequently, the outermost metallic wall is mainly responsible for the MWCNT's polarization. At the same time, the outer wall plays the most important role in the MWCNT/polymer matrix interfacial interaction. Splitting of this wall should inevitably change the interfacial polarization.

Beside the change in the interfacial interaction, other factors might contribute to the observed phenomena. By splitting the MWCNT, it is converted into a cylindrically shaped stack of nanoribbons, similar to a longitudinally cut rubber hose. The unique metallic nanotube components that would contribute to the permittivity, if the MWCNT were intact, no longer exist. Furthermore, because the contour of the MWCNT is open, an electrical field is allowed inside the structure.

As we mentioned above, all of the distribution parameters of the GNRs in the composite appear similar to those of the MWCNTs. The only difference is the nanoscopic structure of the individual inclusions, which likely changes the interfacial polarization between the inclusions and the matrix.

CONCLUSION

We prepared a new composite material made by incorporation of GNRs into a dielectric host matrix. The composite possesses remarkably low loss at reasonably high permittivity values. By varying the content of the conductive filler, one can tune the loss and permittivity to a wide range of desirable values. The obtained data are an example of how nanoscopic changes in the structure of conductive filler and the subsequent change in the interfacial polarization can affect the macroscopic properties of composites.

AUTHOR INFORMATION

Corresponding Author

*E-mail: kempel@egr.msu.edu (L.C.K.); tour@rice.edu (J.M.T.).

ACKNOWLEDGMENT

This work was supported by the AFOSR (FA9550-09-1-0581 and FA9550-09-1-0182) and the Advanced Energy Consortium (Baker Hughes, Halliburton, Conoco Phillips, bp, OXY, Marathon, Shell, Total, Petrobras, Schlumberger). We thank Mitsui Inc. for the MWCNTs kindly supplied via Drs. M. Endo, A. Tanioka, and S. Tsuruoka.

REFERENCES

(1) Baugham, R. H.; Zakhidov, A. A.; de Heer, W. A. *Science* **2002**, *297*, 787–792.
(2) Liu, Z.; Bai, G.; Huang, Yi.; Li, F.; Ma, Y.; Guo, T.; He, X.; Lin, X.; Gao, H.; Chen, Y. *J. Appl. Phys.* **2007**, *111*, 13696–13700.
(3) Shuba, M. V.; Slepyan, G. Y.; Maksimenko, S. A.; Hanson, G. W. *J. Appl. Phys.* **2010**, *108*, 114302–10.
(4) Grimes, C. A.; Mungle, C.; Kouzoudis, D.; Fang, S.; Eklund, P. C. *Chem. Phys. Lett.* **2000**, *319*, 460–464.
(5) Wu, J.; Kong, L. *Appl. Phys. Lett.* **2004**, *84*, 4956–4958.
(6) Grimes, C. A.; Dickey, E. C.; Mungle, C.; Ong, K. G.; Qian, D. *J. Appl. Phys.* **2001**, *90*, 4134–4137.
(7) Xiang, C.; Pan, Y.; Liu, X.; Sun, X.; Shi, X.; Guo, J. *Appl. Phys. Lett.* **2005**, *87*, 123103−1–3.
(8) Higginbotham, A.; Stephenson, J.; Smith, R.; Killips, D.; Kempel, L. C.; Tour, J. M. *J. Phys. Chem. C* **2007**, *111*, 17751–17754.
(9) Laverghetta, T. *Microwave Materials and Fabrication Techniques*, 2nd ed.; Artech House: Boston, 1991.
(10) Kosynkin, D. V.; Lu, W.; Sinitskii, A.; Pera, G.; Sun, Z.; Tour, J. M. *ACS Nano* **2011**, *5*, 968–974.
(11) Ferrari, A. C. *Solid State Commun.* **2007**, *143*, 47–57.
(12) Lespade, P.; Marchand, A. *Carbon* **1984**, *22*, 375–385.
(13) Larachi, F.; Dehkissia, S.; Adnot, A.; Chornet, E. *Energy Fuels* **2004**, *18*, 1744–1756.
(14) Liu, L.; Matitsine, S.; Gan, Y. B.; Chen, L. F.; Kong, L. B.; Rozanov, K. N. *J. Appl. Phys.* **2007**, *101*, 094106–7.
(15) Dang, Z. -M.; Wang, L.; Yin, Y.; Zhang, Q.; Lei, Q. -Q. *Adv. Mater.* **2007**, *19*, 852–857.
(16) Yuan, J.-K.; Li, W.-L.; Yao, S.-H.; Lin, Y.-Q.; Sylvestre, A.; Bai, J. *Appl. Phys. Lett.* **2011**, *98*, 032901–3.
(17) Yuan, J.-K.; Yao, S.-H.; Dang, Z.-M.; Sylvestre, A.; Genestoux, M.; Bai, J. *J. Phys. Chem. C* **2011**, *115*, 5515–5521.
(18) Ebbesen, T. W.; Lezec, H. J.; Hiura, H.; Bennett, J. W.; Ghaemi, H. F.; Thio, T. *Nature* **1996**, *382*, 54–56.